Schweizerischer Erdbebendienst
Service Sismologique Suisse
Servizio Sismico Svizzero
Swiss Seismological Service

ETH
Eidgenössische Technische Hochschule Zürich
Swiss Federal Institute of Technology Zurich

# SITE CHARACTERIZATION REPORT

## **SBUL:** Bulle (FR), Ecole professionnelle

Francesco Panzera, Vincent Peron, Manuel Hobiger, Donat Fäh

Last Modification: 04th July, 2020

Schweizerischer Erdbebendienst (SED)
Service Sismologique Suisse
Servizio Sismico Svizzero
Servizi da Terratrembels Svizzer
ETH Zürich

Sonneggstrasse 5
8092 Zürich
Schweiz
francesco.panzera@sed.ethz.ch

# Contents

# Summary

Bulle (FR), located in the west of Switzerland, was selected as site for the installation of a new station, called SBUL, as part of the renewal project of the Swiss Strong Motion Network (SSMNet). In order to better assess the local underground, we performed site characterization measurements with different techniques. The results of the horizontal-to-vertical spectral ratio (H/V) show curves with a fundamental frequency of about 1.30 Hz, having variable amplitude, and predominant peaks between 12.0 Hz and about 18.0 Hz, related to the presence of a cover of infill with variable thickness in the area of the seismic station. The inversion of the passive seismic array measurements allows us to infer only one main discontinuity at about 3-4 m, separating an upper layer with shear-wave velocity of about 250 m/s and a layer with velocity of about 950 m/s. At depths between 80 and 120 m the velocity jumps to 1750 m/s, possibly related to the presence of a hard rock layer. The $V_{S30}$ value of the site is about 709 m/s, corresponding to soil class B in both EC8 and SIA261. The theoretical shear-wave transfer functions predict an amplification at about 17 Hz, in quite good agreement with the fundamental H/V frequency of the site where the strong motion station is installed.

# 1 Introduction

The station SBUL is part of the Swiss Strong Motion Network (SSMNet). The station has been installed on 2 May 2018 in the framework of the second phase of the Swiss Strong Motion Network (SSMNet) renewal project (Fig. 1). In order to better characterize the underground of the station, we performed passive array measurements.
The site is of interest because is located in a populated area in the central-western Switzerland at the border between the Molasse basin and the Helvetic nappes. Its geographical location improves the network geometry increasing the territory coverage.
The measurement campaign was carried out on 12 April 2019 in order to characterize the soil column in terms of fundamental frequency and shear wave velocity.


*Figure 1: Map showing the location of the strong motion station (red circle) in Bulle. © 2020 swisstopo (JD100042)*

# 2 Geological setting

A geological map of the surroundings of the site in Bulle is shown in Fig. 2, together with the stations of the passive array measurements. The permanent station SBUL and all sixteen stations of the passive array measurement lie on moraine deposit.

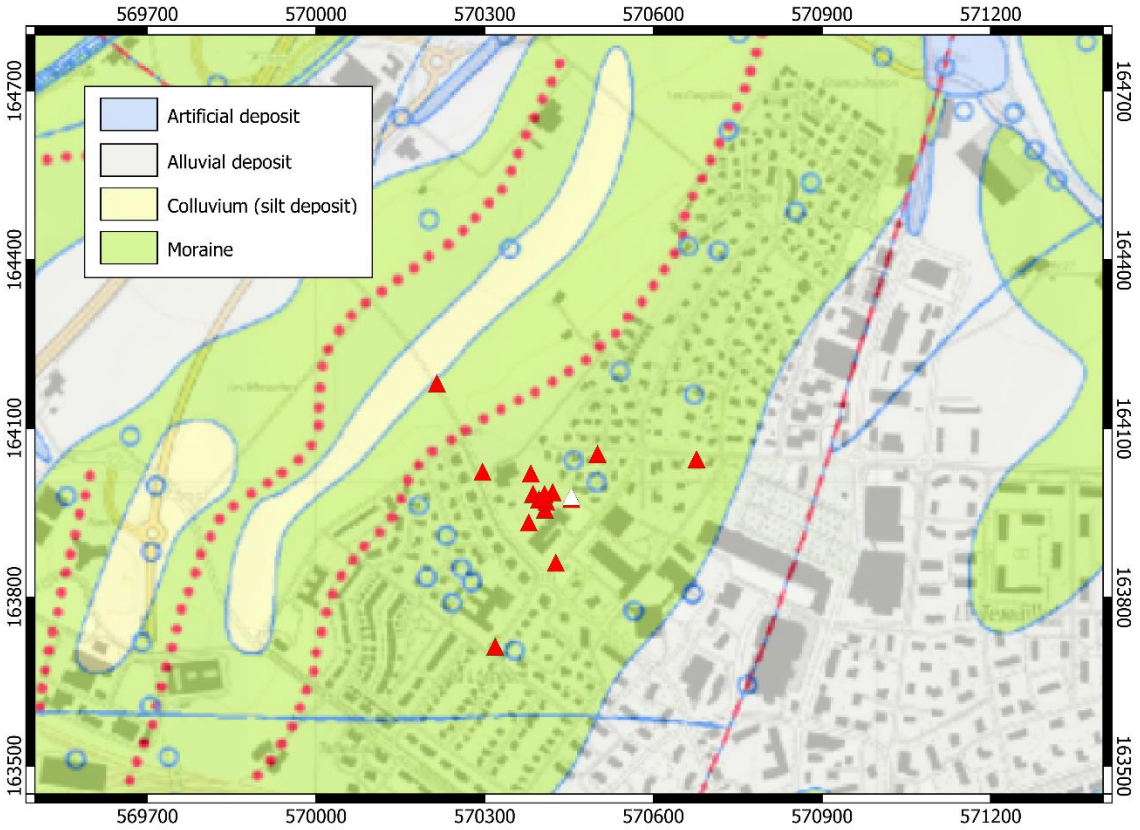


*Figure 2: Geological map of area around station SBUL. The stations of the passive array recordings are indicated by red triangles, whereas SBUL is shown by a white triangle. © 2020 swisstopo (JD100042)*

# 3 Site characterization measurements

## 3.1 Data set

To characterize the deeper underground structure around the seismic station, we performed passive seismic measurements in April 2019 close to the location of SBUL (Fig. 3).

A single array of 16 stations was installed (Fig. 4). The stations were planned to be located on five rings of different radii around a central station. The inner three rings were planned in regular forms with angular distances of 280 between the different stations on the ring. These three rings had radii of 8, 20, and 50 m, respectively. The second and third rings were rotated by 30 degrees with respect to the first and second rings, respectively. These three rings were installed in the field using a measuring tape and a plan of the intended orientations from the central station. The fourth ring was planned to have a distance of 120 m from the central station. The stations of the fifth ring were placed at distances of about 280 m from the array center. The minimum and maximum interstation distances in the finally installed array were 8.0 and 560 m, respectively.

Each station consisted of a Lennartz 5s sensor connected to a Centaur digitizer, where four stations in the central part had two sensors connected to the same digitizer. The station names of the array are composed of "SBU" followed by a three-digit number between 42 and 49, 52 and 55, 65, 67, 74 and 75 (corresponding to the Centaur digitizer serial number for numbers lower than 60 and serial number plus 20 for higher numbers). The array recording time was 140 minutes (8400 s). The station locations have been measured by a differential GPS system (Leica Viva GS10) which was set up to measure with a precision better than 5 cm.

*Figure 3: Seismic station installation example for the measurements in Bulle.*


*Figure 4: Layout of the array measurement in Bulle. The locations of the stations for the passive seismic measurement are indicated by the red triangles. The white rectangle indicates the seismic station. © 2020 swisstopo (JD100042)*

## 3.2 H/V and RayDec ellipticity curves

Figure 5 shows the H/V curves determined with the time-frequency analysis method (Fäh et al., 2009) for all stations of the passive array. The H/V curves are quite homogeneous and show a similar pattern up to 5.0 Hz, with a fundamental frequency of about 1.30 Hz having variable amplitude. This amplitude inconsistency could be related to the variability of the moraine deposit compactness. Above this frequency value, most of the curves are characterized by peaks between 12.0 and about 18.0 Hz. This behavior indicates the presence of a thin near-surface layer with variable thickness.

The RayDec technique (Hobiger et al., 2009) is meant to eliminate the contributions of other wave types than Rayleigh waves and give a better estimate of the ellipticity than the classical H/V technique. The RayDec ellipticity curves for all stations of the array measurements are shown in Figure 5. The RayDec curves of the different stations are similar to the one obtained through H/V, except for station SBU044. This site is characterized by an ellipticity curve with strange behavior (amplitude below 1 from 0.5 Hz to 3.0 Hz).

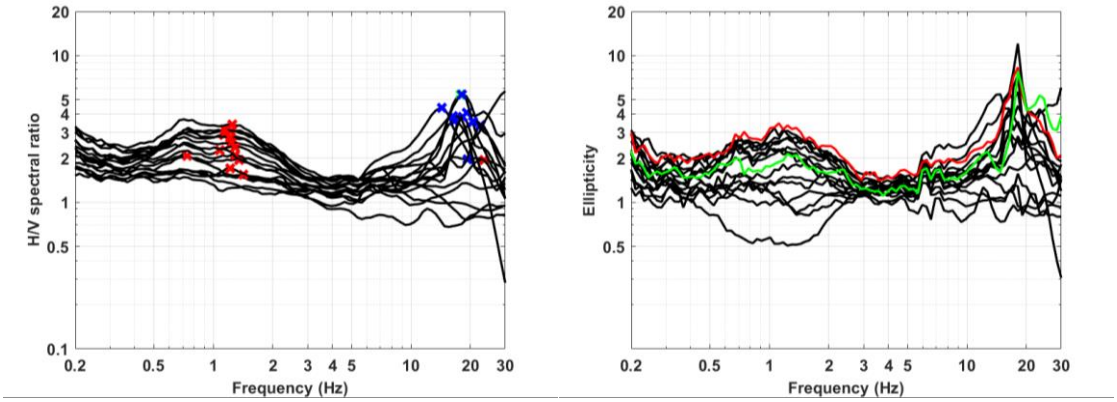


*Figure 5: Left: H/V curves of the different stations of the array measurements in Bulle with picked fundamental frequency (red cross) and secondary peak (blue cross). Right: RayDec ellipticities for all stations of the array. The curve of SBU074, the array center, is highlighted in red, whereas the curve for SBU048, the station closest to SBUL, is highlighted in green.*

### 3.3 Polarization measurements

The polarization analysis was performed according to Burjánek et al. (2010) and Burjánek et al. (2012). The results for all stations of the array are similar. Only the results for SBU048, the station closest to SBUL (see location in Fig. 3), are shown in Fig. 6. The results show that the ground motion is almost linear and horizontally polarized around the high frequency H/V peak (about 18.0 Hz). In the polar plot, no pronounced polarization directions are present.

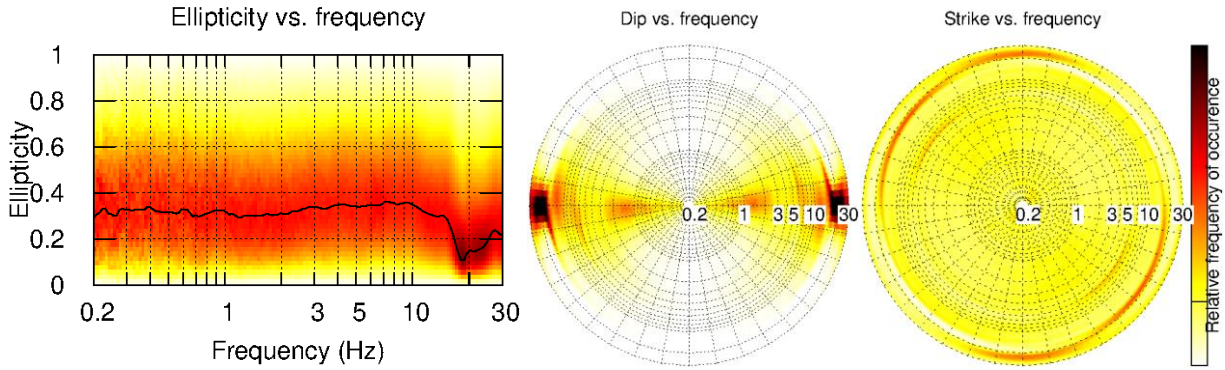


*Figure 6: Polarization analysis of station SBU048.*

### 3.4 3-component high-resolution FK

The results of the 3-component high-resolution FK analysis (Poggi and Fäh, 2010) are shown in Fig. 7. The results on the transverse component show the dispersion curve (DC) of a single Love wave mode from 2.4 to 15.5 Hz. On the radial component one mode is visible in the frequency range from 2.6 to 16.5 Hz. On the vertical component, two possible modes were picked from 2.6 to 19.3 Hz and from 20.0 to 29.1 Hz. The corresponding ellipticity curves of the radial and vertical components are clearly identified in the respective frequency range and do not show strong peaks.

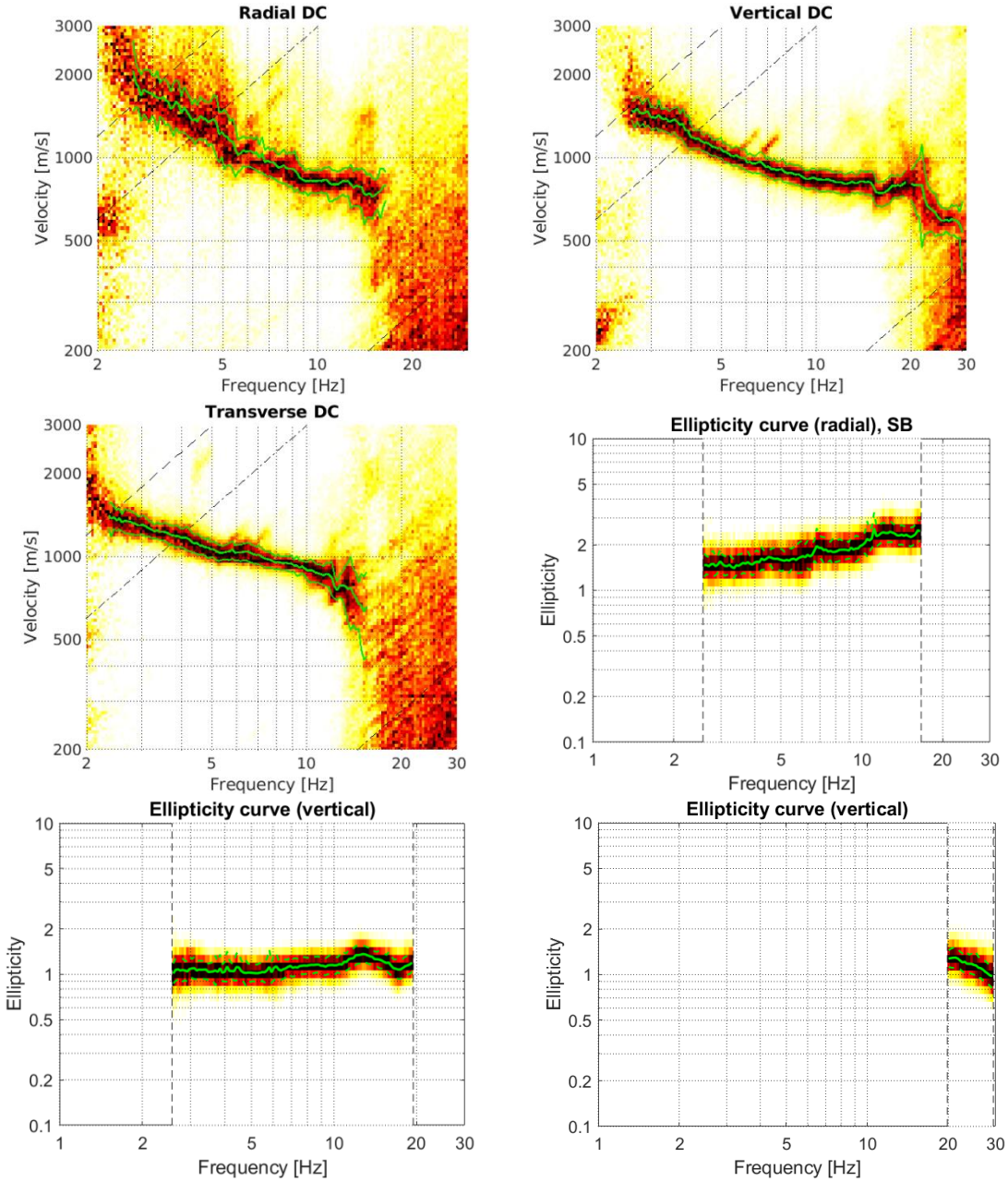


*Figure 7: Dispersion and ellipticity curves for the transverse, radial and vertical components obtained with the 3-component HRFK algorithm (Poggi and Fäh, 2010). The dashed and dotted black lines are the array resolution limits. The solid green lines are picked from the data, where the central line indicates the best value and the two outer lines the standard deviation, respectively.*

### 3.5 WaveDec

The results of the WaveDec (Maranò et al., 2012) processing are shown in Fig. 8. This technique estimates the properties of single or multiple waves simultaneously with a maximum likelihood approach. In order to get good results, the parameter γ has been tuned to modify the sharpness of the wave property estimation between purely maximum likelihood estimation and a Bayesian Information Criterion. Here, a value of $\gamma = 0.2$ was used, corresponding to a mostly maximum likelihood estimation.

Love wave dispersion curves are clearly retrieved between about 2.5 and 13.4 Hz. The Rayleigh wave dispersion curve can be picked between 2.7 Hz and 28.5 Hz. The ellipticity angle for the picked Rayleigh wave dispersion curve is negative from 2.7 to 18.0 Hz, showing retrograde particle motion, and becomes positive above, which is compatible with a singular peak and a change of the particle motion to prograde. The ellipticity curve shows a peak at about 19.0 Hz.

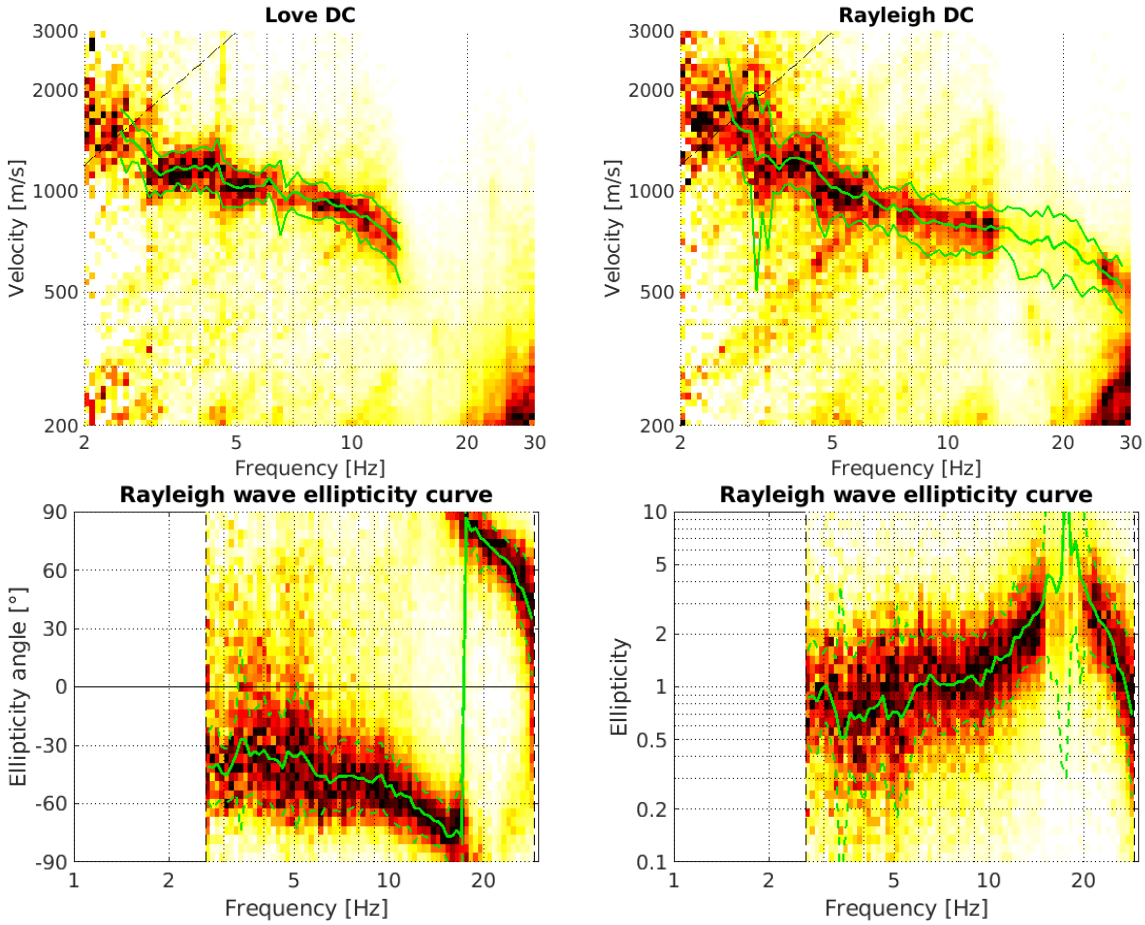


*Figure 8: Dispersion and ellipticity curves for the Love and the Rayleigh waves obtained with WaveDec (Maranò et al., 2012). The solid green lines are picked from the data, where the central line indicates the best value and the two outer lines the standard deviation, respectively.*

### 3.6 Summary

Figure 9 gives an overview of the dispersion and ellipticity curves determined by the different methods. For Love waves, WaveDec gives a dispersion curve that is similar to HRFK, but with phase velocities slightly lower than those observed through HRFK. For Rayleigh waves, all methods are in rather good agreement in the whole covered frequency range.

The ellipticity curves retrieved using the different methods are quite similar. The RayDec curve has a peak at about 19.0 Hz and the WaveDec curve well retrieves this frequency peak. The ellipticity retrieved from the HRFK radial component has the same shape as the RayDec curve in the frequency 2.6-16.5 Hz. Finally, the ellipticity obtained from HRFK on the vertical component is almost flat. From the ellipticity angle, it is possible to observe the change of particle motion from retrograde to prograde at about 19.0 Hz (Fig. 8).

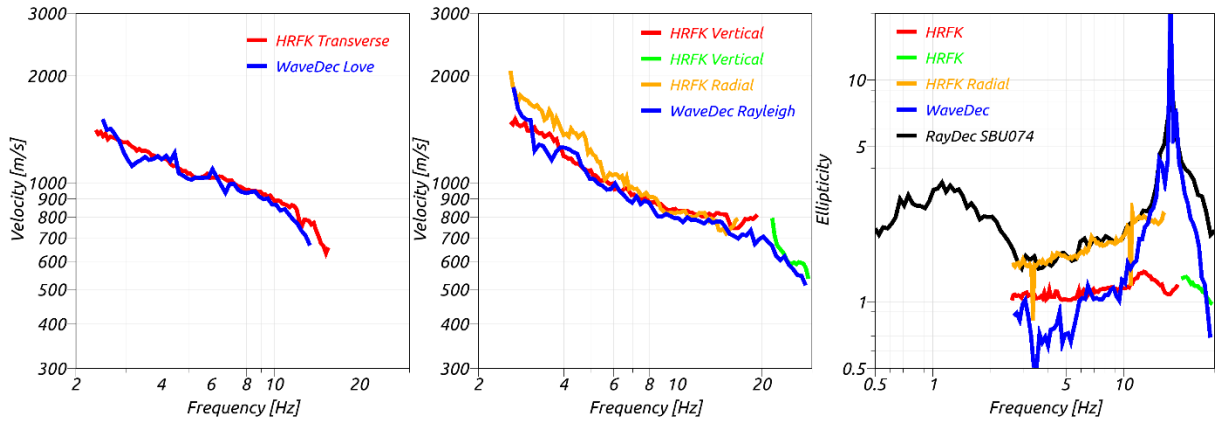


*Figure 9: Comparison between the computed dispersion curves and ellipticity curves. The RayDec curve is related to the measurement point SBU074 array center.*

# 4 Data inversion

## 4.1 Inversion targets

We performed inversions using as much information as possible, by means of different parts of the picked dispersion and ellipticity curves. The details of these inversion targets are indicated in Table 1 and the corresponding curves are shown in Fig. 10.

In the inversion process, the curve derived with HRFK was used as Love wave dispersion curve for the fundamental mode, because it covers a larger frequency range than WaveDec and has lower estimation uncertainties. The vertical component HRFK curve was used as fundamental mode Rayleigh wave dispersion curve. The inversion process was also performed using the WaveDec ellipticity around the peak frequency. This choice was made after several trials considering combinations of the picked experimental ellipticity curves, Love and Rayleigh wave fundamental and higher mode dispersion curves.

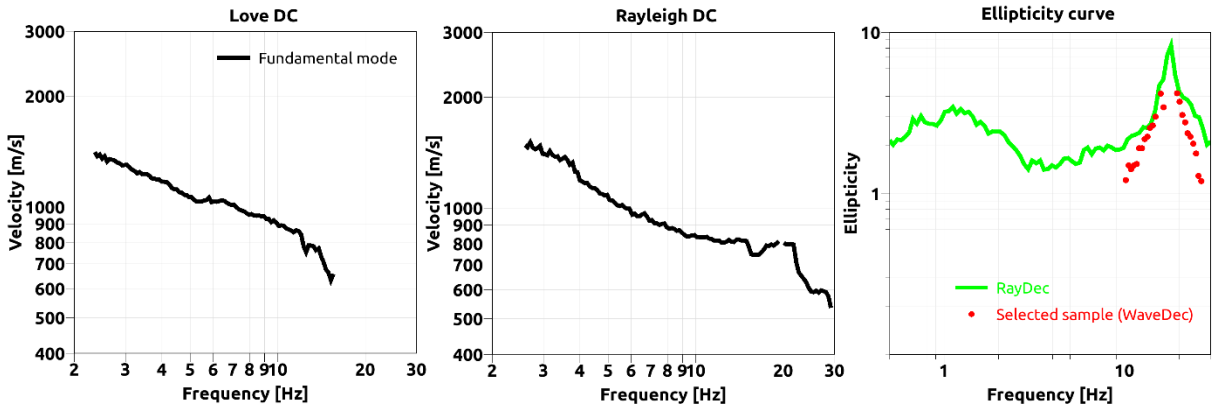


*Figure 10: Overview of the dispersion curves used as targets for the different inversions. The RayDec curve is related to the measurement point SBU074, the array center.*

*Table 1: List of the data curves used as target in the inversion.*

| Method | Wave type | Mode | Curve type | Frequency range [Hz] |
|---|---|---|---|---|
| HRFK (T) | Love | fundamental | dispersion | 2.4 – 15.5 |
| HRFK (V) | Rayleigh | fundamental | dispersion | 2.6 – 19.3 |
| HRFK (V) | Rayleigh | fundamental | dispersion | 20.0 – 29.1 |
| WaveDec | Rayleigh | fundamental | ellipticity | 9.8 – 15.4, 18.8 – 26.6 |

## 4.2 Inversion parameterization

For the inversion, six different parameterizations are used in total. The first five have free values of the depths and velocities of the different layers, ranging from four to eight layers (including half-space). The last parameterization has fixed layer depths and consists of 21 layers in total, with the deepest interface at 160 m depth.

The S- and P-wave velocities are allowed to range from 150 to 3500 m/s and from 200 to 4000 m/s, respectively. The deepest layer interfaces were allowed to range to a depth of 160 m for all parameterizations. The density was fixed to 2300 kg/m$^3$ for the bedrock layer and to 2000 kg/m$^3$ for all other layers.

## 4.3 Inversion results

We performed a total of seven inversions with different parameterizations (see Table 2). Each inversion run produced 200000 total models in order to assure a good convergence of the solution. The results of these inversions are shown in Figs 11 – 16.

*Table 2: List of inversions*

| Inversion | Number of layers | Number of models | Minimum misfit |
|---|---|---|---|
| SBUL 4l | 4 | 200000 | 0.266 |
| SBUL 5l | 5 | 200000 | 0.278 |
| SBUL 6l | 6 | 200000 | 0.266 |
| SBUL 7l | 7 | 200000 | 0.294 |
| SBUL 8l | 8 | 200000 | 0.309 |
| SBUL fix | 15 | 200000 | 0.327 |

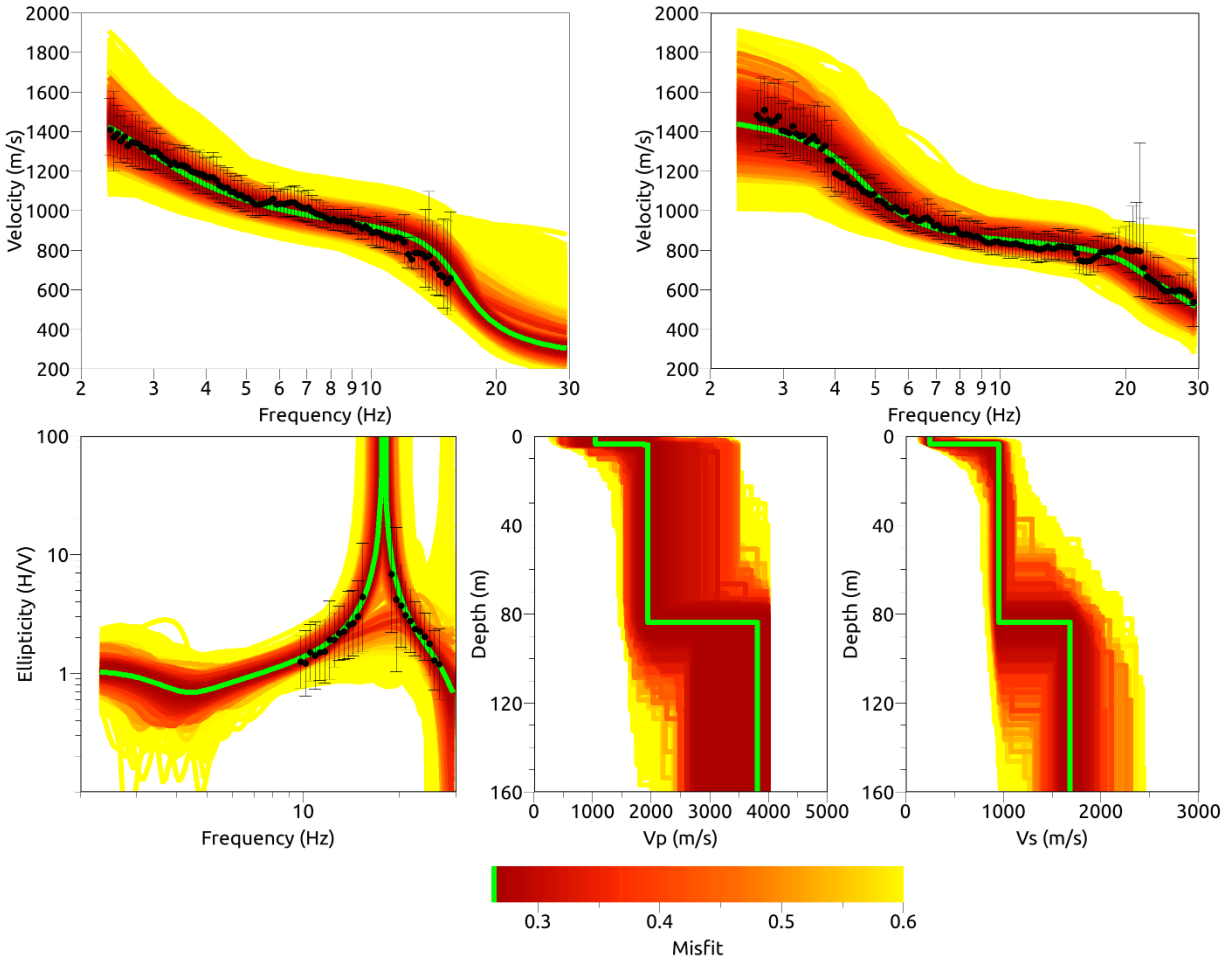


*Figure 11: Inversion* SBUL *4l. Top line: Dispersion curves for the Love wave fundamental mode (left) and the Rayleigh wave fundamental mode (right). Bottom line: Rayleigh wave ellipticity curve (left), P-wave velocity profiles (center) and S-wave velocity profiles (right). The black dots indicate the data points used for the inversion, the green line indicates the best-fitting model.*

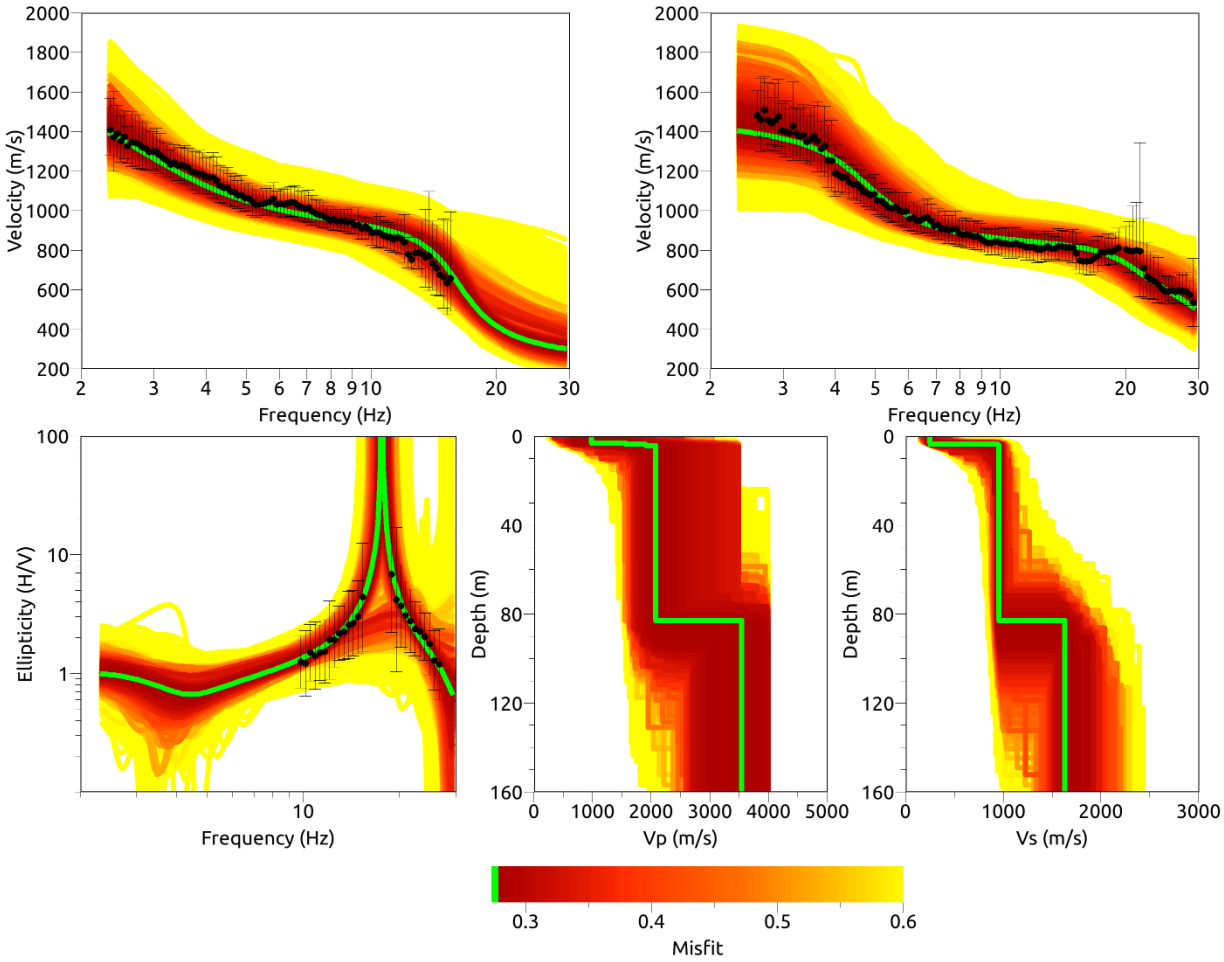


*Figure 12: Inversion* SBUL *5l. Top line: Dispersion curves for the Love wave fundamental mode (left) and the Rayleigh wave fundamental mode (right). Bottom line: Rayleigh wave ellipticity curve (left), P-wave velocity profiles (center) and S-wave velocity profiles (right). The black dots indicate the data points used for the inversion, the green line indicates the best-fitting model.*

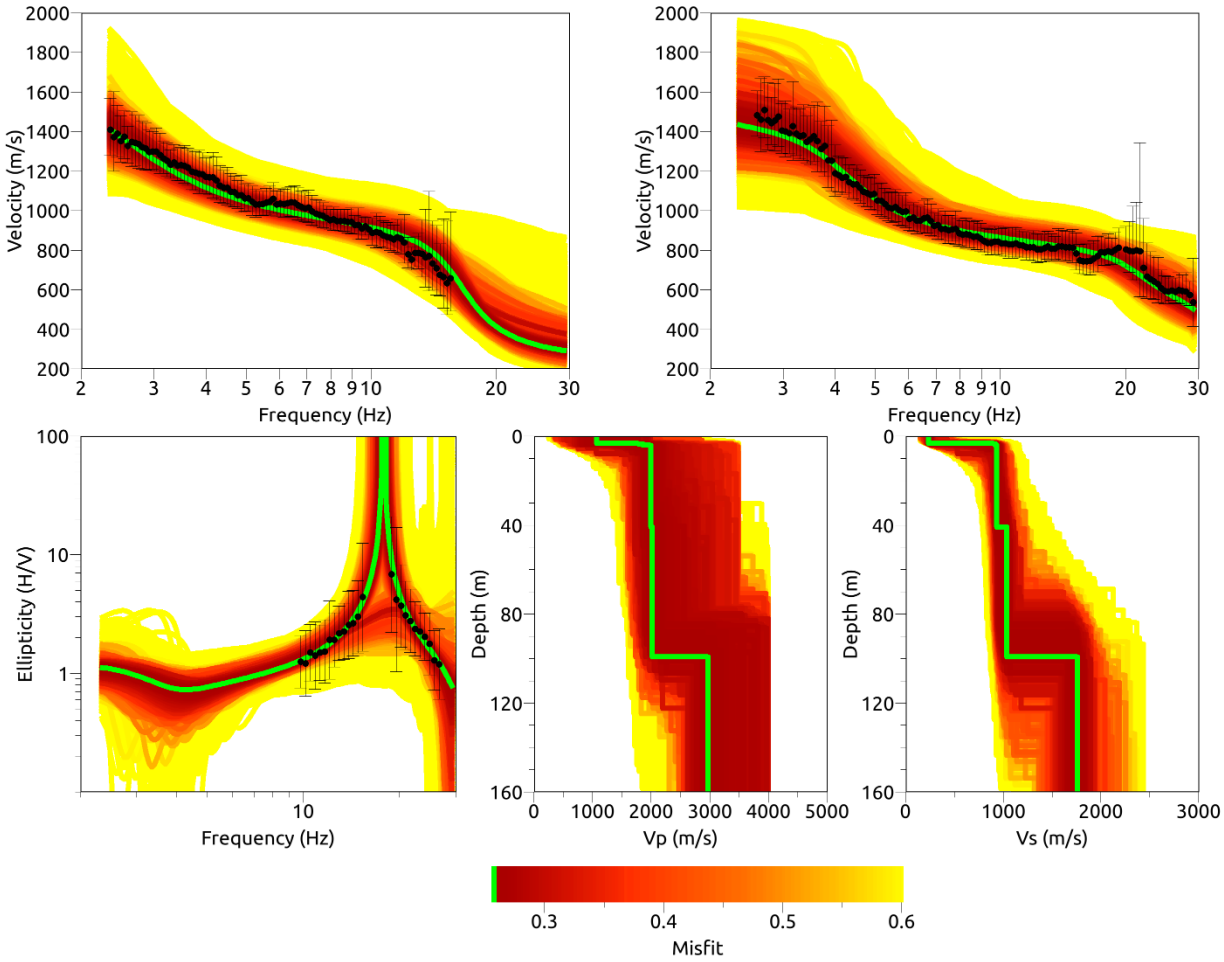


*Figure 13: Inversion* SBUL *6l. Top line: Dispersion curves for the Love wave fundamental mode (left) and the Rayleigh wave fundamental mode (right). Bottom line: Rayleigh wave ellipticity curve (left), P-wave velocity profiles (center) and S-wave velocity profiles (right). The black dots indicate the data points used for the inversion, the green line indicates the best-fitting model.*

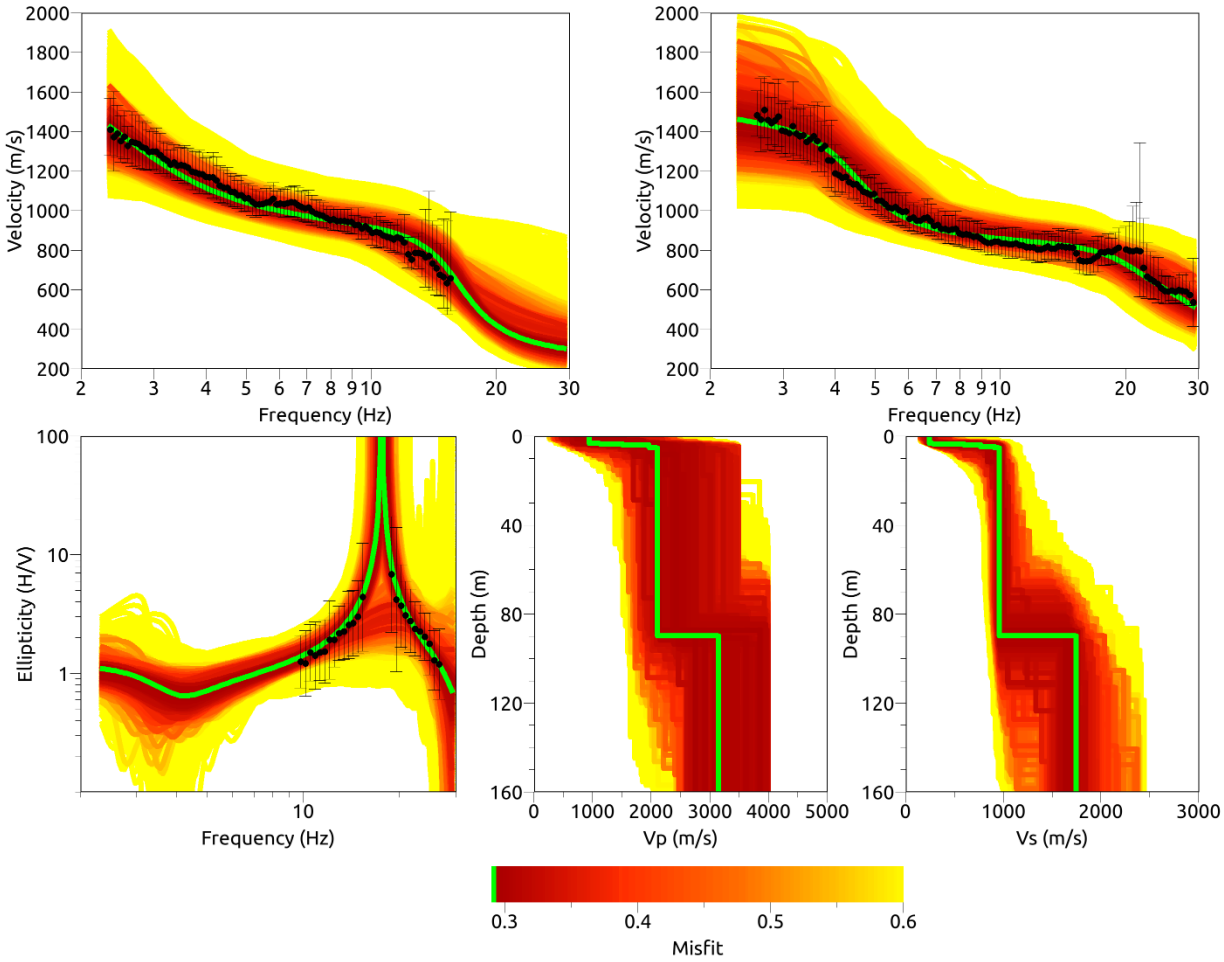


*Figure 14: Inversion* SBUL *7l. Top line: Dispersion curves for the Love wave fundamental mode (left) and the Rayleigh wave fundamental mode (right). Bottom line: Rayleigh wave ellipticity curve (left), P-wave velocity profiles (center) and S-wave velocity profiles (right). The black dots indicate the data points used for the inversion, the green line indicates the best-fitting model.*

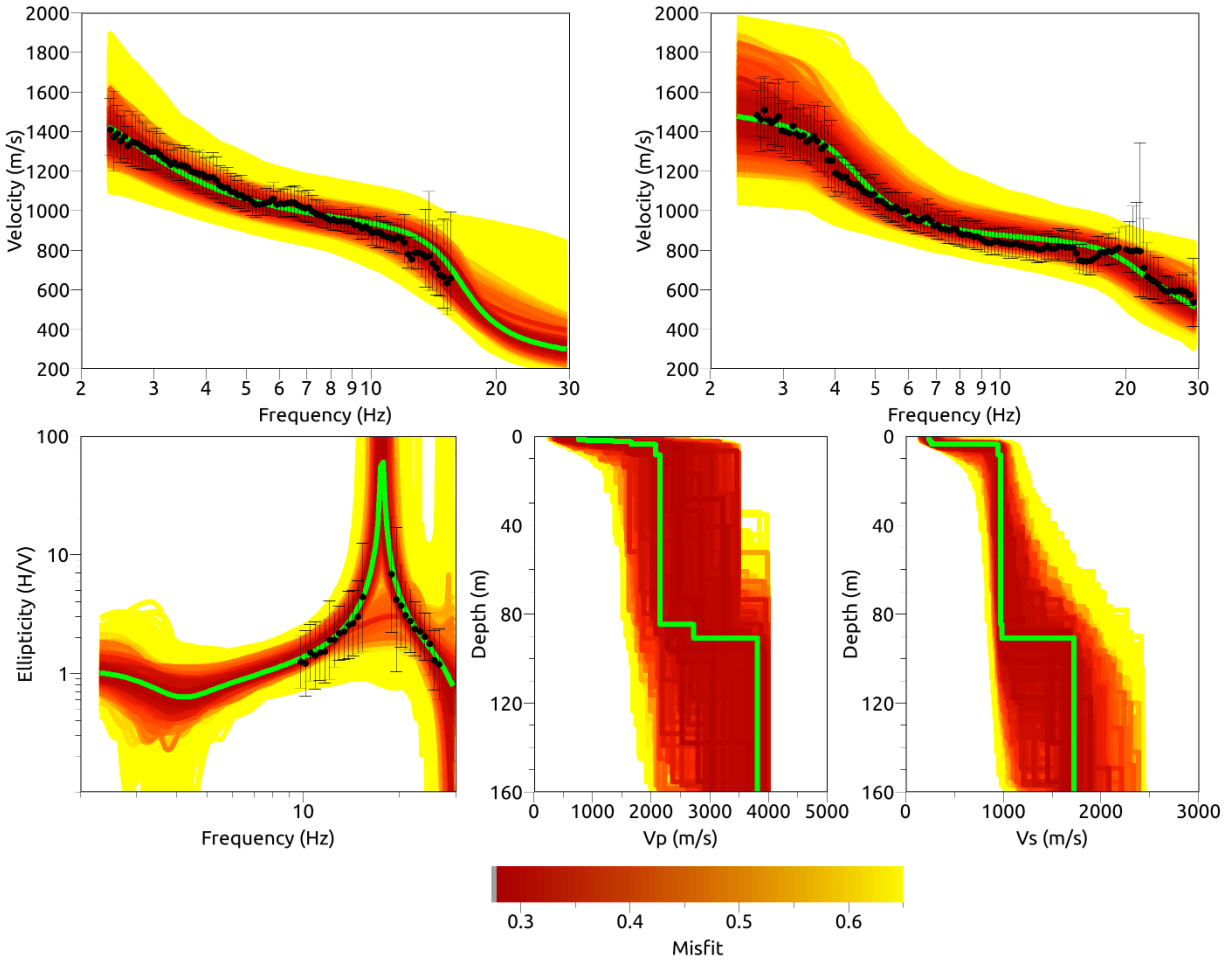


*Figure 15: Inversion* SBUL *8l. Top line: Dispersion curves for the Love wave fundamental mode (left) and the Rayleigh wave fundamental mode (right). Bottom line: Rayleigh wave ellipticity curve (left), P-wave velocity profiles (center) and S-wave velocity profiles (right). The black dots indicate the data points used for the inversion, the green line indicates the best-fitting model.*

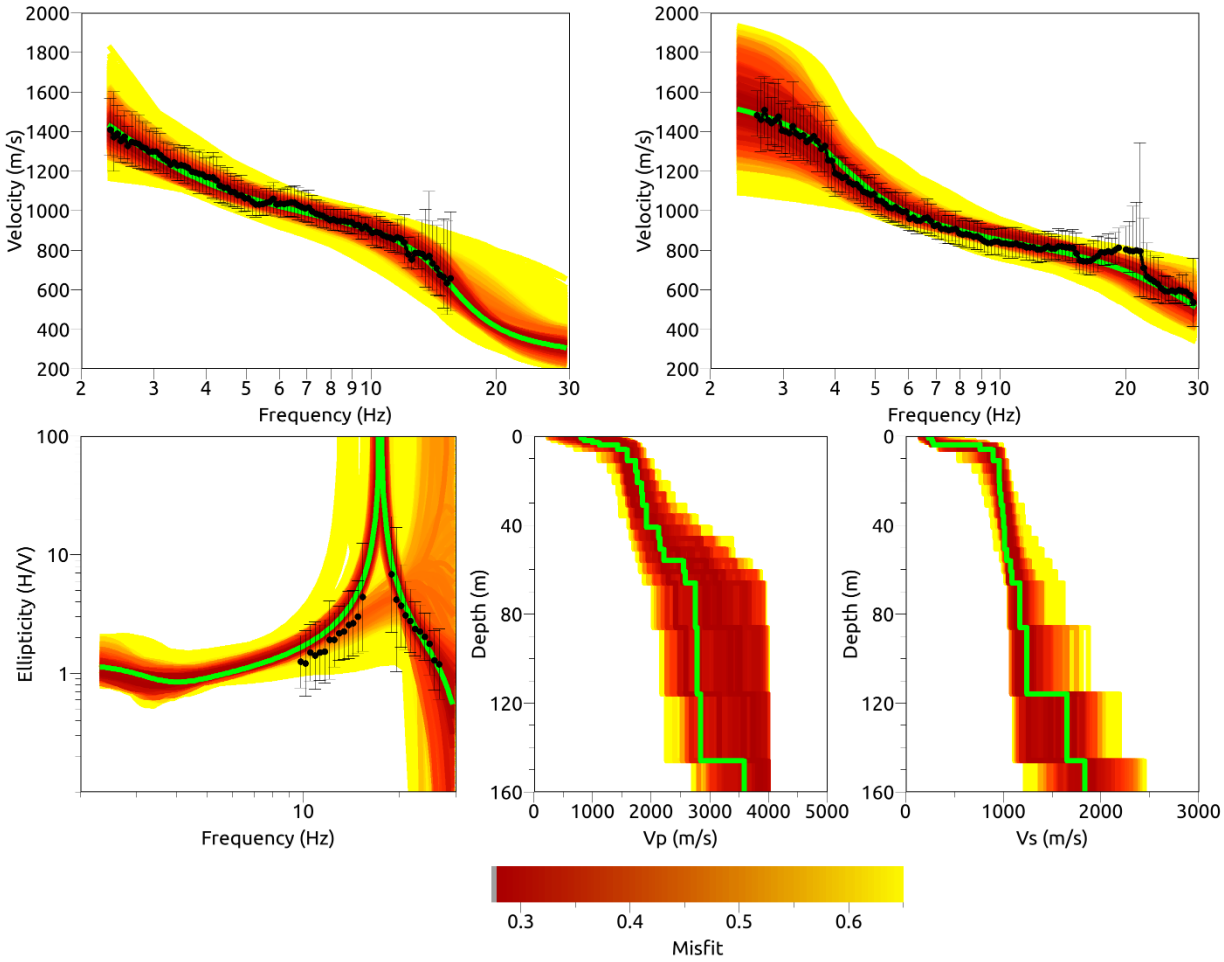


*Figure 16: Inversion* SBUL *fix. Top line: Dispersion curves for the Love wave fundamental mode (left) and the Rayleigh wave fundamental mode (right). Bottom line: Rayleigh wave ellipticity curve (left), P-wave velocity profiles (center) and S-wave velocity profiles (right). The black dots indicate the data points used for the inversion, the green line indicates the best-fitting model.*

### 4.4 Discussion of the inversion results

The best-fitting models of the inversions are shown in Fig. 17. There are several main characteristics that all models have in common. The seismic bedrock is found at depths between 80 and 120 m, with a shear wave velocity of about 1750 m/s. The variability in depth of this discontinuity is probably due to the lack of information below 2.5 Hz in our experimental curves. Above the bedrock, only one main discontinuity is visible at about 3-4 m, which separates an upper layer with velocity of about 250 m/s and a lower one with velocity of about 950 m/s. At about 80-120 m the velocity jumps to 1750 m/s, possibly related to the presence of a hard rock layer at depth. The velocity profiles resulting from the different inversions have $V_{S30}$ values between 699.1 and 713.5 m/s, with an average value of 709.2 ± 7.6 m/s.

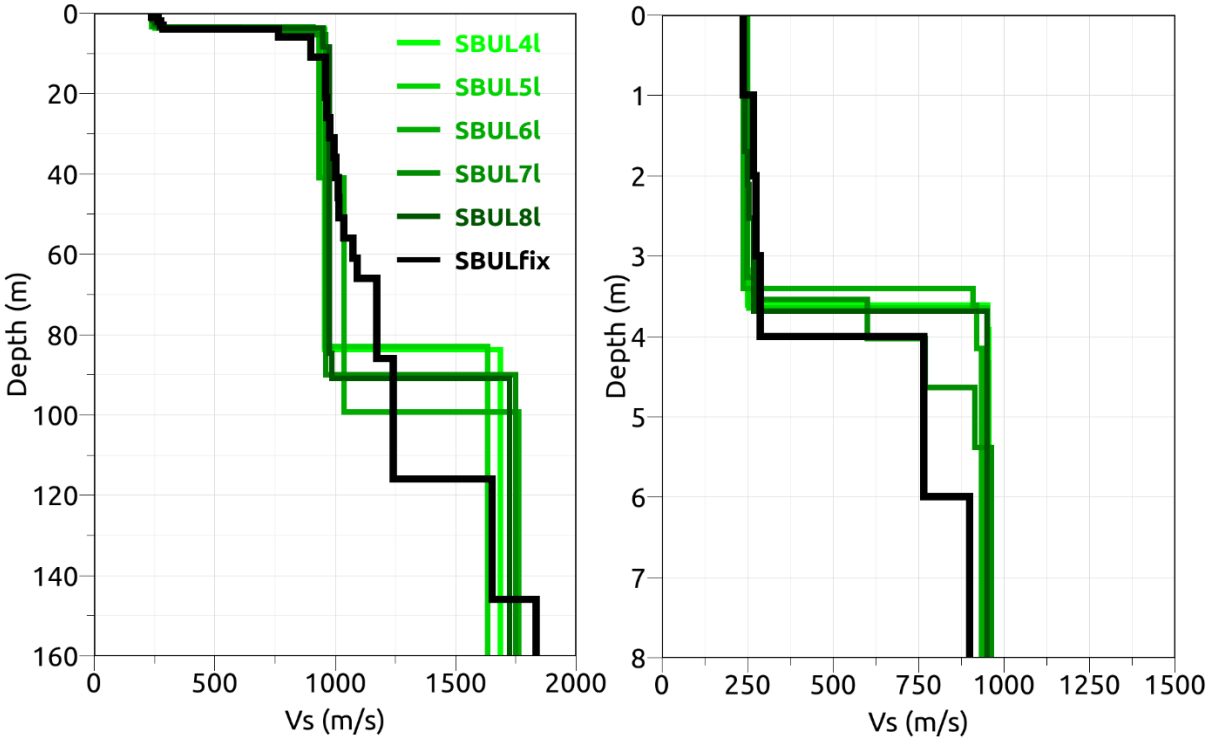


*Figure 17: Overview of the shear-wave velocity profiles of the different inversions (left) and zoom on the upper 8 m of the inversion profiles (right).*

# 5 Further results from the inverted profiles

## 5.1 SH transfer function

In Figure 18, the average theoretical SH-amplification relative to the Swiss reference rock profile from the obtained models is compared to the empirical amplification obtained at station SBUL for (about 30) earthquake recordings. In this case, the models are predicting an amplification up to a factor of 5.0 at about 17.0 Hz, slightly lower than the peak of the empirical amplification. The present empirical amplification is not stable considering the low number of earthquakes used for its computation, but a quite good agreement is observed especially at high frequency. As soon as the station has recorded a sufficient number of earthquakes, the comparison will be made again.

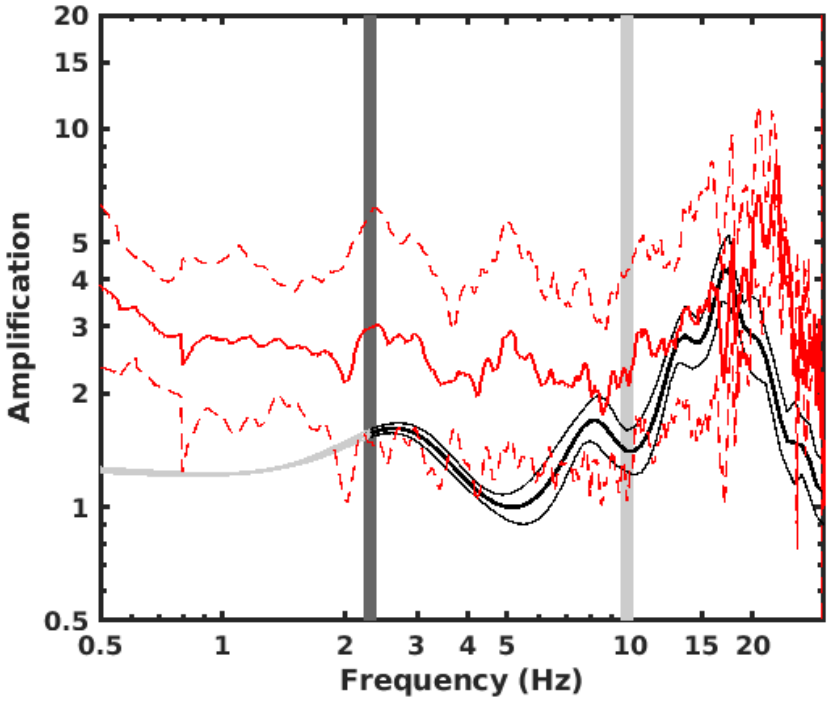


*Figure 18: Modeled amplification function for the best velocity models of the six inversions (black). The red continuous line is the average empirical amplification function at station SBUL, whereas the dashed red lines are the standard deviations.*

## 5.2 Quarter-wavelength representation

The quarter-wavelength velocity approach (Joyner et al., 1981) provides, for a given frequency, the average velocity at a depth corresponding to 1/4 of the wavelength of interest (Fig. 19). The results using this proxy, considering frequency limits of the experimental data of 2.4 to 29.1 Hz for the dispersion curves, is well constrained above 85 m. The quarter wavelength impedance-contrast introduced by Poggi et al. (2012) is also displayed in the figure. It corresponds to the ratio between two quarter-wavelength average velocities, respectively from the top and the bottom part of the velocity profile, at a given frequency.

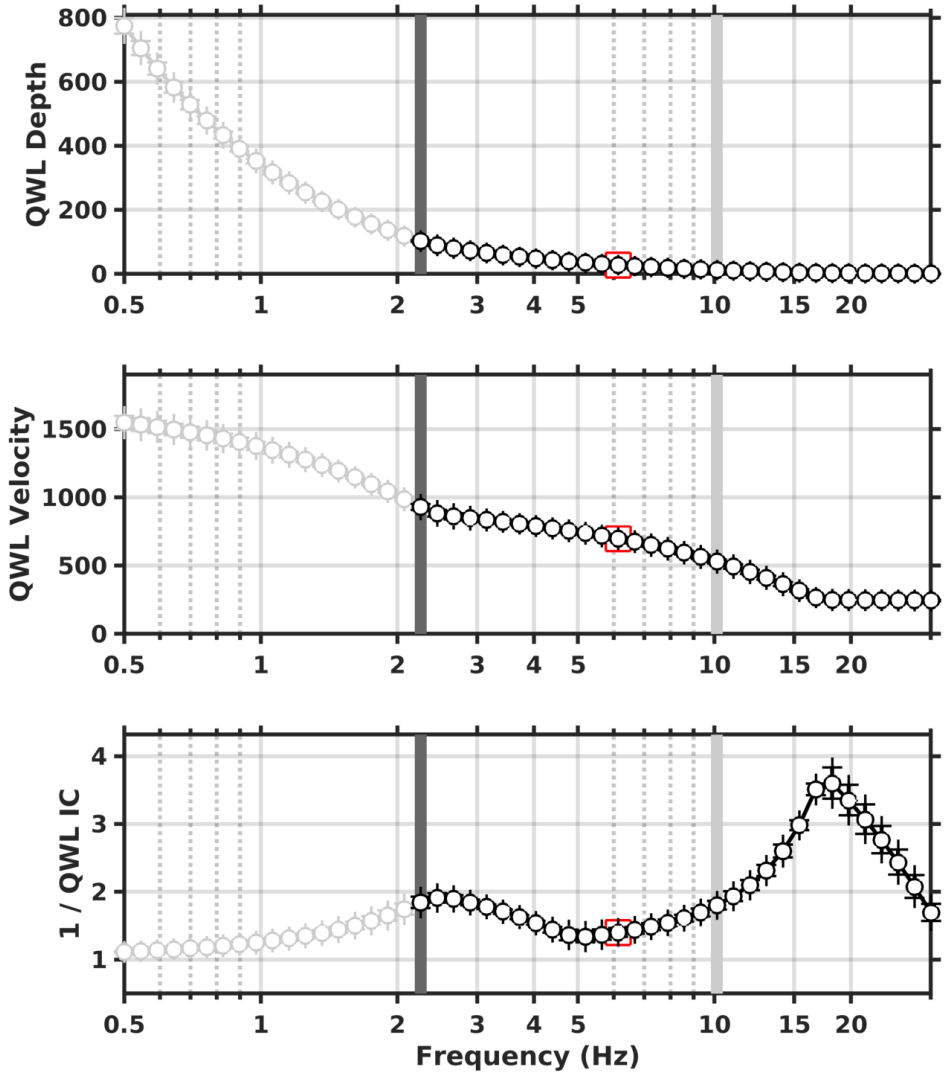


*Figure 19: Quarter wavelength representation of the velocity profiles for the best models of the inversions (top: depth, center: velocity, bottom: inverse of the impedance contrast). The grey light bar shows ellipticity lower frequency value, dark grey bar indicates lower frequency value obtained with dispersion curves and red square corresponds to $f_{30}$ (frequency related to the depth of 30 m).*

# 6 Discussion and conclusions

The H/V analysis points out that the fundamental peak observed at the different stations is at about 1.30 Hz, but showing variable amplitude. This amplitude inconsistency could be related to the variability of the compactness of the moraine deposits. The predominant frequency peaks are instead observed at frequencies ranging between 12.0 and about 18.0 Hz. This behavior is probably linked to the presence of a thin infill of deposits in the area with variable thickness. The inversion of the passive seismic array measurements yields a velocity profile with two main interfaces at about 4 m and 80-120 m. In particular, the upper layer has a velocity of 250 m/s and the second layer is then present with a velocity of about 950 m/s. At about 80-120 m, the velocity jumps to 1750 m/s, possibly related to the bedrock. The depth of the bedrock is not well constrained due to the lack of information at frequency lower than 2.4 Hz in our dispersion curves (a seen in the QWL depth). The $V_{S30}$ value of the site is determined as about 709 m/s, corresponding to soil class B in EC8 and in SIA261 classifications.
The theoretical shear-wave transfer function predicts an amplification factor of 5 at about 17.0 Hz, in quite good agreement with the 18 Hz fundamental frequency of the site where the strong motion station is installed. The comparison was also made with observations at this station showing a quite good agreement especially at high frequency.

# Acknowledgements

The authors thank Franziska Glüer and David Farsky for their help during the measurements.

# References

Burjánek, J., Gassner-Stamm, G., Poggi, V., Moore, J. R., and Fäh, D. (2010). Ambient vibration analysis of an unstable mountain slope. Geophys. J. Int., 180:820–828.

Burjánek, J., Moore, J. R., Molina, F. X. Y., and Fäh, D. (2012). Instrumental evidence of normal mode rock slope vibration. Geophys. J. Int., 188:559–569.

Fäh, D., Gardini, D., et al. (2003). Earthquake Cataloque of Switzerland (ECOS) and the related macroseismic database. Eclogae geol. Helv. 96.

Fäh, D., Wathelet, M., Kristekova, M., Havenith, H., Endrun, B., Stamm, G., Poggi, V., Burjanek, J., and Cornou, C. (2009). Using ellipticity information for site characterisation. NERIES deliverable JRA4 D4, available at http://www.neries-eu.org.

Fritsche, S., Fäh, D., Gisler, M., and Giardini, D. (2006). Reconstructing the damage field of the 1855 earthquake inSwitzerland: historical investigations on a well-documented event Geophys. J. Int. (2006)166, 719–731

Hobiger, M., Bard, P.-Y., Cornou, C., and Le Bihan, N. (2009). Single station determination of Rayleigh wave ellipticity by using the random decrement technique (RayDec). Geophys. Res. Lett., 36.

Maranò, S., Reller, C., Loeliger, H.-A., and Fäh, D. (2012). Seismic waves estimation and wavefield decomposition: Application to ambient vibrations. Geophys. J. Int., 191:175–188.

Poggi, V. and Fäh, D. (2010). Estimating Rayleigh wave particle motion from three component array analysis of ambient vibrations. Geophys. J. Int., 180:251–267.

Poggi, V., Edwards, B., and Fäh, D. (2010). Characterizing the Vertical-to-Horizontal Ratio of Ground Motion at Soft-Sediment Sites. Bulletin of the Seismological Society of America, 102(6): 2741 2756.